

# H I 21 cm opacity fluctuations power spectra towards Cassiopeia A

Nirupam Roy <sup>1\*</sup>, Jayaram N. Chengalur <sup>2\*</sup>, Prasun Dutta <sup>3\*</sup> and Somnath Bharadwaj <sup>3\*</sup>

<sup>1</sup>National Radio Astronomy Observatory, 1003 Lopezville Road, Socorro, NM 87801, USA

<sup>2</sup>National Centre for Radio Astrophysics, TIFR, Post Bag 3, Ganeshkhind, Pune 411 007, India

<sup>3</sup>Department of Physics and Meteorology & Centre for Theoretical Studies, IIT Kharagpur, Kharagpur 721 302, India

Accepted yyyy month dd. Received yyyy month dd; in original form yyyy month dd

## ABSTRACT

The angular power spectrum of H I 21 cm opacity fluctuations is a useful statistic for quantifying the observed opacity fluctuations as well as for comparing these with theoretical models. We present here the H I 21 cm opacity fluctuation power spectrum towards the supernova remnant Cas A from interferometric data with spacial resolution of  $5''$  and spectral resolution of  $0.4 \text{ km s}^{-1}$ . The power spectrum has been estimated using a simple but robust visibility based technique. We find that the power spectrum is well fit by a power law  $P_\tau(U) = U^\alpha$  with a power law index of  $\alpha \sim -2.86 \pm 0.10$  ( $3\sigma$  error) over the scales of  $0.07 - 2.3 \text{ pc}$  for the gas in the Perseus spiral arm and  $0.002 - 0.07 \text{ pc}$  ( $480 - 15730 \text{ au}$ ) for that in the Local arm. This estimated power law index is consistent with earlier observational results based on both H I emission over larger scales and absorption studies over a similar range of scales. We do not detect any statistically significant change in the power law index with the velocity width of the frequency channels. This constrains the power law index of the velocity structure function to be  $\beta = 0.2 \pm 0.6$  ( $3\sigma$  error).

**Key words:** MHD — ISM: general — ISM: individual (Cas A) — ISM: structure — radio lines: ISM — turbulence

## 1 INTRODUCTION

It is now well established that the H I 21 cm opacity in the Galaxy shows measurable small scale structure. Very Long Baseline Interferometry (VLBI) observations show opacity fluctuations on angular scales as small as 20 milli arc seconds corresponding to a projected separation  $\sim 10 \text{ au}$ , if one assumes that the opacity variations occur in a thin screen (Brogan et al. 2005). Similarly, multi-epoch observations of some high velocity pulsars show evidence for H I 21 cm opacity variation on scales of 5 - 100 au (Frail et al. 1994). Several other pulsars however do not show opacity variations (Johnston et al. 2003), leading to suggestions that the occurrence of fine scale structure in the Galaxy may be rare. Much of these observed fluctuations on au scales were earlier believed to originate in H I “clouds” with densities  $\sim 10^4 - 10^5 \text{ cm}^{-3}$ . It is hard to explain the existence of such structures in equilibrium with other, orders of magnitude lower density, components of the diffuse interstellar medium (ISM). Deshpande (2000) has shown that the observed small scale transverse variations have contributions from structure on all scales and that the fluctuations at larger spatial scales could, in projection, produce the measured small scale fluctuations. Conversely, there are other observational and numerical simulation results supporting the existence of tiny scale structures which have a size of  $\sim 3000 \text{ au}$ , with a density of  $\sim$

$100 \text{ cm}^{-3}$  (e.g. Braun & Kanekar 2005; Vázquez-Semadeni et al. 2006; Hennebelle & Audit 2007). With an evaporation timescale of  $\sim 1 \text{ Myr}$ , these structures can survive only if the ambient pressure is much higher than the normal value or if they are formed continuously on a comparable timescale. Details regarding their origin and physical properties are, however, still not understood. On somewhat larger scales, Deshpande et al. (2000) measured opacity variations of the H I absorption across Cassiopeia A and Cygnus A, and found that the power spectrum of these fluctuations could be fairly well represented by a power law. The slope of the power law was similar for the absorption in the Perseus arm (towards Cas A) and the Outer arm (towards Cygnus A), but substantially different for that from absorption towards Cygnus A arising in the Local arm.

The scale free behavior of fluctuation power spectra of a variety of tracers (H I 21 cm emission intensity, dust emission) is the main observational evidence for the existence of turbulence in the atomic ISM. The slope of the power law of H I 21 cm emission and absorption in our own Galaxy, H I 21 cm emission from the Large Magellanic Cloud, the Small Magellanic Cloud and DDO 210 are all  $\sim -3$  (Crovisier & Dickey 1983; Green 1993; Stanimirović et al. 1999; Elmegreen et al. 2001; Begum et al. 2006). Recently Dutta et al. (2009a,b) have reported that the H I 21 cm intensity fluctuation power spectra for a sample of dwarf and nearby spiral galaxies have a power law index of  $\sim -2.6$  and  $\sim -1.5$  on scales respectively smaller and larger than the scale height of the galaxy disk. This is interpreted as the effect of a transition from three dimensional to two dimensional

\* E-mail: nroy@aoc.nrao.edu (NR); chengalu@ncra.tifr.res.in (JNC); prasun@cts.iitkgp.ernet.in (PD); somnath@cts.iitkgp.ernet.in (SB)

turbulence at scales larger than the disk thickness. The observed fractal structure of H I in several dwarf galaxies in the M 81 group is also consistent with the self-similar hierarchical structure of the turbulent ISM without any preferred length scale (Westpfahl et al. 1999).

On the theoretical side, fine scale structure in the neutral gas is naturally expected in turbulent models of the ISM. The fluctuations in the H I 21 cm opacity in a particular velocity range depend on the fluctuations in the density, spin temperature and velocity of the gas. Deshpande et al. (2000) show that in the case of small fluctuations of density, the dependence on temperature is small. Turbulence however, gives rise to fluctuations in both the density and velocity of the gas and both of these contribute to the observed opacity fluctuations. Lazarian & Pogosyan (2000) show that the slope of the observed power spectrum changes depending on whether the H I 21 cm emission is averaged over a velocity range that is large (“thick slices”) or small (“thin slices”) compared to the turbulent velocity dispersion. Observations with high enough spectral resolution can hence disentangle the statistical properties of the velocity and the density fluctuations.

Cassiopeia A or Cas A (G111.7–2.1) is in the constellation Cassiopeia in the Galactic second quadrant. It is a shell type supernova remnant of diameter  $5'$  at a distance of approximately 3.4 kpc (Reed et al. 1995), and is one of the brightest radio sources in the sky (flux density of  $\sim 2720$  Jy at 1 GHz). The radio images show it to have a clear shell like structure along with compact emission knots, the shell thickness estimated from the radial brightness profile is  $\sim 30''$ . There have been many studies of the ISM towards Cas A using H I 21 cm absorption (e.g. Clark et al. 1962; Clark 1965; Schwarz et al. 1986; Bieging et al. 1991; Reynoso et al. 1997) and a variety of other tracers like H<sub>2</sub>CO and OH (Goss et al. 1984; Bieging & Crutcher 1986) all of which reveal small scale structure. A recently developed formalism for statistically robust extraction of the fluctuation power spectrum from interferometric data is used here to re-examine the issue and to constrain the H I 21 cm opacity fluctuation power spectrum towards Cas A. This method is particularly useful because one can completely avoid the complications of deconvolution and imaging the strong background source. We note that the opacity power spectrum towards Cas A has been obtained earlier by Deshpande et al. (2000). They used the data from the Very Large Array (VLA) B, C and D configurations but with only 18 antennas in each configuration due to software restrictions. Estimating the power spectrum using the visibility based formalism for the same line of sight will allow us to compare the results from two very different methods to cross-check different techniques. Section §2 briefly describes the data while our methods of estimating the intensity and opacity fluctuation power spectra are outlined in Section §3 and §4 respectively. Section §5 contains the results and discussion, and we present conclusions in Section §6.

## 2 DATA

The Giant Metrewave Radio Telescope (GMRT) L-band (21 cm) receiver was used to observe the H I in absorption towards supernova remnant Cas A. The observation was carried out on December 03, 2006 and the total duration was about 13 hours with on-source time of about 8 hours. VLA calibrator sources 2148+611 and 2355+498 were used for phase calibration. One of the phase calibrators was observed for 3 minutes for every 20 minutes observation of Cas A. Standard flux calibrators 3C48 and 3C286 were

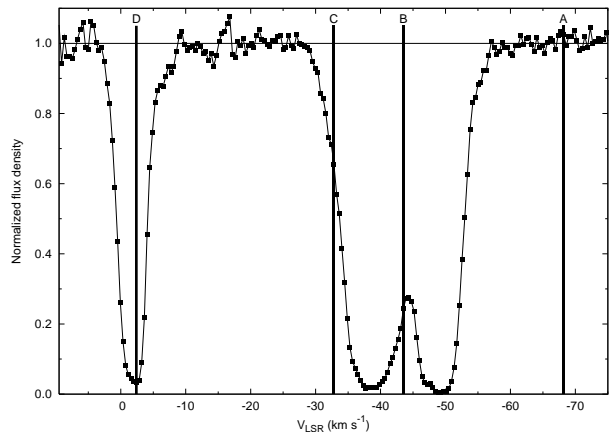


**Figure 1.** Integrated H I 21 cm absorption spectrum towards the supernova remnant Cas A. The continuum corresponds to the total flux density of Cas A. The wide feature at negative LSR velocity is the absorption produced by gas from the Perseus spiral arm and the absorption near zero LSR velocity is from the Local arm gas. Power spectra for channels marked as A, B, C and D are shown in Figure 2.

observed for about 20 minutes in every 4 hours during the observation. Frequency switching was used to calibrate the spectral baseline — the flux calibrator scans (which were also used for bandpass calibration) were observed at frequency offset by 5 MHz from that of the absorption line. A total baseband bandwidth of 0.5 MHz divided into 256 frequency channels centered at 1420.5973 MHz was used for the observation. This corresponds to a velocity resolution of  $\sim 0.4$  km s<sup>-1</sup> per channel and the total bandwidth was sufficient to cover the H I 21 cm absorption produced by gas both from the Perseus arm and the Local arm. Data analysis was carried out using standard AIPS. After flagging out bad data, the flux density scale, instrumental phase and frequency response were calibrated. The calibrated visibility data of Cas A were then used to estimate the angular power spectra and the errors. The integrated H I 21 cm absorption spectrum towards Cas A derived from the GMRT observation is shown in Figure (1). The wide feature at negative velocity with respect to the Local Standard of Rest (LSR) is the absorption produced by gas from the Perseus spiral arm and the absorption near zero LSR velocity is from the Local arm gas.

## 3 THE INTENSITY FLUCTUATION POWER SPECTRUM

The angular power spectrum  $P_S(U)$  of the sky brightness fluctuations  $\delta S(l, m)$ , is the Fourier transform of the autocorrelation function  $\xi_S$

$$P_S(U) \equiv P_S(u, v) = \int \int \xi_S(l, m) e^{-2\pi i(ul+vm)} dl dm. \quad (1)$$

Here  $(l, m)$  refer to the directions on the sky,  $(u, v) \equiv \vec{U}$  refer to the inverse angular separation and  $\xi_S$  is given by

$$\xi_S(l - l', m - m') = \langle \delta S(l, m) \delta S(l', m') \rangle. \quad (2)$$

The angular bracket refers to an ensemble average over different realisations of  $\delta S(l, m)$  which is assumed to be stochastic in nature. The fluctuations are also assumed to be statistically isotropic which implies that  $P_S(U)$  depends only on  $U = |\vec{U}|$ .

The visibility  $\mathcal{V}_\nu(\vec{U})$  measured in radio interferometric observations directly probes a Fourier mode of the sky brightness fluctuation

tuation  $\delta S(l, m)$ . Here the inverse angular scale  $\vec{U}$  directly corresponds to a baseline, the antenna separation projected in the plane perpendicular to the direction of observation, measured in units of the observing wavelength  $\lambda$ . It is common practice to express the dimensionless quantity  $\vec{U}$  in units of kilo wavelength ( $k\lambda$ ). The Fourier relation between  $\mathcal{V}_\nu(\vec{U})$  and  $\delta S(l, m)$  allows us to identify each baseline with an inverse angular scale, and to directly estimate the angular power spectrum from the measured visibilities.

Detailed discussions of the visibility based power spectral estimator that we use here can be found in Begum et al. (2006) and Dutta et al. (2009a). Briefly, the estimator  $\hat{P}(\vec{U}) = \langle \mathcal{V}_\nu(\vec{U}) \mathcal{V}_\nu^*(\vec{U} + \Delta\vec{U}) \rangle$ , is obtained by correlating every visibility  $\mathcal{V}_\nu(\vec{U})$  with all other nearby visibilities  $\mathcal{V}_\nu^*(\vec{U} + \Delta\vec{U})$ , i.e. those which lie within the disk defined by  $|\Delta\vec{U}| < (\pi\theta_0)^{-1}$ , where  $\theta_0$  is the angular radius of the source. In the case of Cas A,  $\theta_0 \sim 2.5'$ , i.e. the angular radius of the source. Since the fluctuations are assumed to be statistically isotropic, the correlations are averaged over different  $\vec{U}$  directions to obtain the final estimator. To increase the signal to noise ratio we further average the estimator in bins of  $U$ . Dutta et al. (2009a) show that the expectation value of the estimator  $\hat{P}(\vec{U})$  is the convolution of the power spectrum  $P(U)$  with a window function  $|\tilde{W}_\nu(U)|^2$ . The window function, which quantifies the effect of the finite angular extent of the source, is peaked around  $U = 0$  and has a width of order  $(\pi\theta_0)^{-1}$  beyond which  $|\tilde{W}_\nu(U)|^2 \sim 0$ . For the optically thin shell-type geometry of Cas A the convolution does not effect the shape of the power spectrum beyond a baseline  $U_m \approx 1.6 k\lambda$  (Roy et al. 2009), and we may directly interpret the real part of the estimator  $\hat{P}(\vec{U})$  as the power spectrum  $P(U)$ . The estimator  $\hat{P}(\vec{U})$  also has a small imaginary component arising mainly from noise. We compute the  $1\sigma$  error bars for the estimated power spectrum by assuming the error to be the quadrature sum of contributions from two sources of uncertainty, viz. the sample variance and the system noise. At small  $U$  the uncertainty is dominated by the sample variance which comes from the fact that we have a finite and limited number of independent estimates of the true power spectrum. At large  $U$ , it is dominated by the system noise in each visibility.

The longest baseline in our observation ( $\sim 25$  km) corresponds to an angular resolution of  $\sim 2.5''$ , but our power spectrum estimation is restricted to  $U \leq 50 k\lambda$  (angular scale  $\sim 5''$ ) because the larger baselines do not have an adequate signal to noise ratio. Similarly for  $U \leq 1.6 k\lambda$  (angular scale  $\sim 2.5'$ ) the sample variance leads to large uncertainties in the power spectral estimate. Note that since the estimator is local in  $U$ , the estimate of the power spectrum over this specific range in  $U$  is not affected by the missing zero spacing baselines or the cut-off at large  $U$ . Certainly these cut-offs and consequent Gibbs phenomena will produce significant ringing and distortion in the image. However, since the power spectrum is estimated directly in the  $uv$  plane, our method, unlike image based techniques, has completely avoided these problems.

Figure 2 shows the estimated power spectrum for four different channels with H I absorption features of different optical depth. Note that since channel A has no H I absorption, it just shows intensity fluctuations power spectrum of the background source Cas A. On the other hand, channel D has inadequate signal to noise to constrain the power spectrum due to very large optical depth. The power spectrum  $P_{I_c}$  of the continuum emission from Cas A, seen in the channels without H I absorption, has been studied in Roy et al. (2009). This power spectrum is well fit by a broken power law

$$\begin{aligned} P_{I_c} &= CU^{-2.22} \quad \text{for } U < 10.6 \text{ k}\lambda \\ &= 10.6^{1.01} CU^{-3.23} \quad \text{for } U > 10.6 \text{ k}\lambda \end{aligned} \quad (3)$$

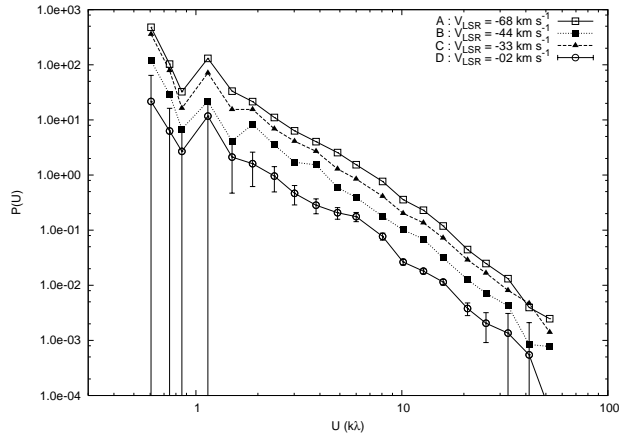


**Figure 2.** Power spectra for channels marked as A, B, C and D in Figure 1. Typical error bars are plotted for only one channel for clarity. Since channel A has no H I absorption, it just shows intensity fluctuations power spectrum of the background source Cas A. Channel D has inadequate signal to noise to constrain the power spectrum due to very large optical depth. Model fit to the data of channel C ( $V_{\text{LSR}} = -33 \text{ km s}^{-1}$ ) is shown in Figure 3.

which has been interpreted as arising from magnetohydrodynamic turbulence in this shell type supernova remnant. The angular scale of the break in the power spectrum corresponds to the shell thickness of Cas A (Roy et al. 2009).

#### 4 THE OPACITY FLUCTUATION POWER SPECTRUM

The sky brightness  $S(l, m)$  towards the extended source Cas A may be written as

$$S(l, m) = I_c(l, m) e^{-\tau(l, m)} \quad (4)$$

where  $I_c(l, m)$  is the continuum radiation from Cas A and  $\tau(l, m)$  is the optical depth for absorption by intervening H I. We expect  $I_c(l, m)$  and  $\tau(l, m)$  to be independent, whereby we can write

$$\xi_S = \langle I_c(l, m) I_c(l', m') \rangle \times \langle e^{-\tau(l, m)} e^{-\tau(l', m')} \rangle. \quad (5)$$

Both  $I_c(l, m)$  and  $\tau(l, m)$  can be decomposed into the sum of a constant average value and the fluctuation around that value (as a function of  $l, m$ )

$$\begin{aligned} I_c(l, m) &= I_c^0 + \delta I_c(l, m) \\ \tau(l, m) &= \tau^0 + \delta\tau(l, m) \end{aligned} \quad (6)$$

and hence equation (5) can be re-written as

$$\xi_S = (I_c^{02} + \xi_{I_c}) \times e^{-2\tau^0} \langle e^{-\delta\tau(l, m)} e^{-\delta\tau(l', m')} \rangle \quad (7)$$

where  $\xi_{I_c}$  is the autocorrelation function of continuum intensity fluctuation. Further, we assume that the opacity fluctuation  $\delta\tau$  is a Gaussian random field with zero mean, variance  $\sigma_\tau^2$  and autocorrelation function  $\xi_\tau$ , whereby

$$\langle e^{-\delta\tau(l, m)} e^{-\delta\tau(l', m')} \rangle = \exp(\sigma_\tau^2 + \xi_\tau). \quad (8)$$

The opacity power spectrum  $P_\tau = \mathcal{F}(\xi_\tau)$ , which is our main interest in this paper, is the Fourier transform of  $\xi_\tau$ . The power spectrum of the brightness fluctuations for a frequency channel with H I absorption can be written as

$$P_S = \mathcal{F}\{\xi_S\} = e^{-2\tau^0 + \sigma_\tau^2} (I_c^{02} + P_{I_c}) \otimes \mathcal{F}\{e^{\xi_\tau}\} \quad (9)$$

where  $P_{I_c}$  is the power spectrum of brightness fluctuations of the continuum emission, i.e. the Fourier Transform of  $\xi_{I_c}$ . Equation (9) relates  $P_S$  to the convolution of  $(I_c^{02} + P_{I_c})$  and  $\mathcal{F}\{e^{\xi_\tau}\}$  which refer to the continuum and the H I opacity respectively. It should be noted that while the terms  $P_S$ ,  $P_{I_c}$  and  $\mathcal{F}\{e^{\xi_\tau}\}$  are all functions of  $\vec{U}$ , the terms  $I_c^0$  and  $e^{-2\tau^0 + \sigma_\tau^2}$  do not have any  $\vec{U}$  dependence. In our analysis we have treated  $B = e^{-2\tau^0 + \sigma_\tau^2}$  as a free parameter that determines the amplitude of  $P_S$ . The terms  $I_c^{02}$  and  $P_{I_c}$ , that refer to the continuum radiation, are known from Cas A's total continuum flux density and analysis of the brightness fluctuations in the line free channels (i.e. eq. 3) respectively. The H I opacity power spectrum  $P_\tau$ , which is the quantity that we wish to determine in this analysis, enters eq. (9) through the term  $\mathcal{F}\{e^{\xi_\tau}\}$ . We have assumed that the opacity power spectrum is a power law

$$P_\tau = \mathcal{F}\{\xi_\tau\} = AU^\alpha. \quad (10)$$

Under this assumption the brightness power spectrum  $P_S(U)$  is completely determined by three parameters  $A$ ,  $B$  and  $\alpha$ . For each velocity channel that shows H I absorption we have used standard chi-square minimization to determine the value of these three parameters for which our model prediction (eqs. 9 and 10) best fits the measured  $P_S$ . The values of  $A$  and  $B$  are not of particular interest in the present analysis. Hence we derive only the best fit value of  $\alpha$  and marginalize over  $A$  and  $B$  to estimate errors for  $\alpha$ .

## 5 RESULTS AND DISCUSSION

Figure 3 shows the measured  $P_S$  and the best fit model of  $P_S$  for a single channel with H I absorption. We find that our model, which assumes a power law H I opacity power spectrum (eq. 10), provides a good fit to the measured sky brightness power spectrum  $P_S$ . The reduced chi-square values for the best fit model are, however, not close to 1.0 but are about 0.3. This is most probably because of an overestimation of the errors in the measured  $P_S$ . The estimated errors, for example, are found to be significantly more than the variation of the continuum power spectra across line free channels. It implies that the very conservative and approximate error estimates adopted here may result in a smaller value of the reduced chi-square even when the model represents the observed power spectrum quite well. Hence, we have scaled down the errors of the observed  $P_S$  so that the reduced chi-square is close to 1.0. The  $1\sigma$  errors of the power law index correspond to a change of the reduced chi-square by +1 from its minimum value.

The velocity channels with very strong absorption do not have adequate signal to noise to constrain the power spectrum. On the other hand, for a few channels with dominant continuum signal and very weak H I absorption, the power spectrum does not deviate significantly from the ‘‘continuum’’ power spectrum, making it hard to constrain the opacity spectrum. The optimal channels for this analysis are hence those with moderate H I absorption, where there is still sufficient signal to noise ratio, and the total power spectrum has been significantly modified by the H I absorption. We note that any image-based method of estimating the power spectrum will also be constrained to the same optimal channels by the signal to noise considerations mentioned here.

The best fit value of  $\alpha$  is found to be  $-2.86 \pm 0.30$  ( $3\sigma$  error) for the angular scale of  $5 - 150''$  probed in this observation. Note that this error bar is based on the quadrature sum of the estimated noise due to ‘‘cosmic variance’’ and the signal to noise ratio on each visibility. As discussed above, this is likely to be an overestimate of the true error. Consistent with this, the channel

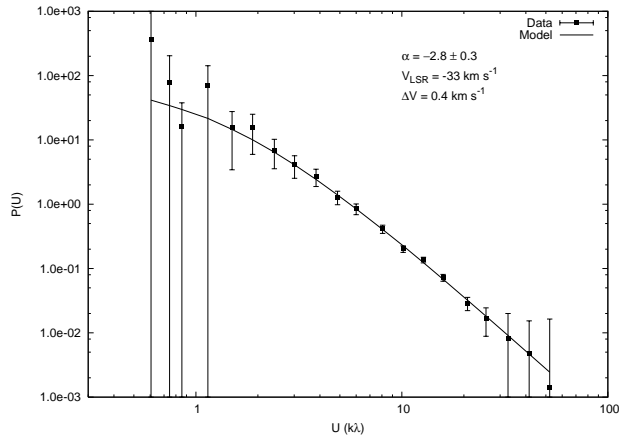


**Figure 3.** Intensity fluctuation power spectrum for a ‘‘thin’’ velocity channel with H I absorption (channel C marked in Figure 1 and Figure 2). The best fit model power spectrum is plotted with the data points.

to channel variation of the best fit value of  $\alpha$  is much less than the estimated error of 0.30. Computing the variance over independent estimates of  $\alpha$  derived for different velocity channels leads to  $\alpha \approx -2.86 \pm 0.10$  ( $3\sigma$  error). We find no significant difference in  $\alpha$  between the velocity channels with absorption produced by gas from the Perseus arm and from the Local arm. The angular scales that our power spectral estimator is valid for corresponds to a linear scale of  $0.07 - 2.3$  pc for the Perseus arm (for an assumed distance of 3 kpc to the arm). The Local arm is  $\sim 100$  pc wide in the solar neighbourhood (Porcel et al. 1998). So, for the Local arm, the upper limit of linear scale range (adopting a distance of 100 pc to the absorbing gas) is  $0.002 - 0.07$  pc ( $480 - 15730$  au). We note that, for the Local arm towards Cygnus A, Deshpande et al. (2000) have reported  $\alpha = -2.5$ , an index somewhat shallower than what we find here, or what those authors find for the Perseus arm and the Outer arm. For the Perseus arm towards Cas A, Deshpande et al. (2000) report  $\alpha = -2.75 \pm 0.25$  ( $3\sigma$  error) for a similar range of linear scales. This factor of  $\sim 2.5$  smaller uncertainty in the current measurement is partly due to the better sensitivity of the present observations and partly due to using a more optimal estimator of the power spectrum. The value of  $\alpha$  that we find here is also consistent with the value ( $\sim -3$ ) reported from the Galactic H I emission observations (Green 1993) probing the scales of  $50 - 200$  pc.

For power law opacity fluctuations power spectrum (eq. 10) with  $-2 \geq \alpha \geq -4$ , the opacity fluctuation smoothed over a length-scale  $x$  is predicted (Deshpande 2000) to have a rms  $\sigma_\tau(x) \propto x^{\frac{\alpha-2}{2}}$  which is also a power law. Using our best fit model we have  $\sigma_\tau(x) = 2.0 (x/4 \text{ pc})^{0.43}$ . Extrapolating this power law, the rms opacity variation is  $\sim 0.05$  on scales of 100 au which is broadly consistent with recent VLA and VLBA studies (Faison et al. 1998; Deshpande et al. 2000; Faison & Goss 2001; Brogan et al. 2005; Lazio et al. 2009). The present study of H I absorption, combined with this result derived from H I emission observations at larger linear scales indicates that there is no significant change in the slope of the power spectrum over 4 – 5 orders of magnitude in linear scale. This spectrum is significantly shallower than the Kolmogorov spectrum (with power law index of  $11/3$ ) expected from an incompressible turbulent medium (Kolmogorov 1941). This may be because of the fact that the turbulence in H I is compressible and magnetohydrodynamic in nature (see Roy et al. 2009, for discussion on this issue).

If the density fluctuation is small compared to the mean density, then for gas in pressure equilibrium, the slope of the opacity fluctuation power spectrum will be nearly the same as that of the density fluctuation power spectrum (Deshpande et al. 2000). However, fluctuations in both the density and velocity fields contribute to the observed H I opacity fluctuations. It can be shown that for the power spectrum estimated from “thick slices”, i.e. those with velocity width larger than the turbulent velocity dispersion, the contribution is only from the density fluctuations, and all velocity information get averaged out (Lazarian & Pogosyan 2000). So, for “thick slices”, the intensity fluctuation is dominantly due to density fluctuation and the observed power law index  $n$  is expected to be same as the index of the density fluctuation power spectrum. On the other hand, for “thin slices”, the power law index of the observed power spectrum is  $n + \beta/2$ , where  $\beta$  is the power law index of the velocity structure function. Hence, it is possible to decouple the density and velocity fluctuations from the power spectra derived from “thin” and “thick” velocity channels. Lazarian & Pogosyan (2000) reported a near-Kolmogorov power law index for both density and velocity fluctuations power spectra for the Milky Way and the Small Magellanic Cloud by applying this technique to the H I emission data (Green 1993; Stanimirović et al. 1999). For our data, we find that though there is a very weak trend of smaller  $\alpha$  for larger channel width, the observed change of  $\alpha$  by about  $-0.1$  for a change of velocity width from  $\sim 0.4$  to  $\sim 12.8 \text{ km s}^{-1}$  is within the  $1 \sigma$  error bar. Since  $\alpha$  remains unchanged for “thin slices” with velocity width as small as  $\sim 0.4 \text{ km s}^{-1}$ , i.e. much smaller than the typical value of  $4.0 \text{ km s}^{-1}$  for turbulent dispersion in Galactic cold H I (Radhakrishnan et al. 1972), we can constrain  $\beta$  to be  $0.2 \pm 0.6$  ( $3\sigma$  error). This is consistent with the value of  $\beta = 2/3$  predicted for turbulence in an incompressible medium (Kolmogorov 1941).

## 6 CONCLUSIONS

In this work, we have studied the H I 21 cm opacity fluctuation towards Cas A. A simple but robust method of directly estimating the power spectrum from the observed visibilities is outlined. In this analysis we avoid the complications of imaging the bright, extended continuum source, of subtracting the continuum and of making optical depth image for channels with H I absorption.

We have found that the H I opacity fluctuation power spectrum can be modelled as a power law with an index of  $-2.86 \pm 0.10$  ( $3\sigma$  error). This is consistent with earlier observational results. We have not found any significant difference of the power law index between velocity channels with absorption produced by the gas from the Perseus arm and the Local arm. We have also checked, by smoothing the visibility data for adjacent channels, if there is variation of the power law index with the velocity width of channels. It is found that, within the estimation errors, the power law index remains constant for a wide range of velocity widths. We can not, however, rule out contribution of velocity fluctuations to the observed opacity fluctuations if the power law index of the velocity structure function is  $0.2 \pm 0.6$  ( $3\sigma$  error). We plan to apply, in future, this visibility based method to study the opacity fluctuations for other lines of sight in different regions of the Galaxy.

## ACKNOWLEDGEMENTS

We thank the staff of the GMRT who have made these observations possible. PD would like to acknowledge HRDG CSIR and

SRIC, IIT, Kharagpur for providing financial support. S.B. would like to acknowledge financial support from BRNS, DAE through the project 2007/37/11/BRNS/357. We are grateful to Rajaram Nityananda and Sanjit Mitra for many helpful comments. We are also grateful to the anonymous referee for prompting us into substantially improving this paper.

## REFERENCES

- Begum A., Chengalur J. N., Bhardwaj S., 2006, MNRAS, 372, L33  
 Bieging J. H., Crutcher R. M., 1986, ApJ, 310, 853  
 Bieging J. H., Goss W. M., Wilcots E. M., 1991, ApJS, 75, 999  
 Braun R., Kanekar N., 2005, A&A, 436, L53  
 Brogan C. L., Zauderer B. A., Lazio T. J., Goss W. M., DePree C. G., Faison M. D., 2005, AJ, 130, 698  
 Clark B. G., Radhakrishnan V., Wilson R. W., 1962, ApJ, 135, 151  
 Clark B. G., 1965, ApJ, 142, 1398  
 Crovisier J., Dickey J. M., 1983, A&A, 122, 282  
 Deshpande A. A., 2000, MNRAS, 317, 199  
 Deshpande A. A., Dwarakanath K. S., Goss W. M., 2000, ApJ, 543, 227  
 Dutta P., Begum A., Bharadwaj S., Chengalur J. N., 2009a, MNRAS, 397, L60  
 Dutta P., Begum A., Bharadwaj S., Chengalur J. N., 2009b, MNRAS, 398, 887  
 Elmegreen B. G., Kim S., Staveley-Smith L., 2001, ApJ, 548, 749  
 Faison M. D., Goss W. M., Diamond P. J., Taylor G. B., 1998, AJ, 116, 2916  
 Faison M. D., Goss W. M., 2001, AJ, 121, 2706  
 Frail D. A., Weisberg J. M., Cordes J. M., Mathers C., 1994, ApJ, 436, 144  
 Goss W. M., Kalberla P. M. W., Dickel H. R., 1984, A&A, 139, 317  
 Green D. A., 1993, MNRAS, 262, 327  
 Hennebelle P., Audit E., 2007, A&A, 465, 431  
 Johnston S., Koribalski B., Wilson W., Walker M., 2003, MNRAS, 341, 941  
 Kolmogorov A., 1941, Dokl. Akad. Nauk SSSR, 31, 538  
 Lazarian A., Pogosyan D., 2000, ApJ, 537, 720  
 Lazio T. J. W., Brogan C. L., Goss W. M., Stanimirović S., 2009, AJ, 137, 4526  
 Porcel C., Garzón F., Jiménez-Vicente J., Battaner E., 1998, A&A, 332, 71  
 Radhakrishnan V., Murray J. D., Lockhart P., Whittle R. P. J., 1972, ApJS, 24, 15  
 Reed J. E., Hester J. J., Fabian A. C., Winkler P. F., 1995, ApJ, 440, 706  
 Reynoso E. M., Goss W. M., Dubner G. M., Winkler P. F., Schwarz U. J., 1997, A&A, 317, 203  
 Roy N., Bharadwaj S., Dutta P., Chengalur J. N., 2009, MNRAS, 393, L26  
 Schwarz U. J., Troland T. H., Albinson J. S., Bregman J. D., Goss W. M., Heiles Carl, 1986, ApJ, 301, 320  
 Stanimirović S., Staveley-Smith L., Dickey J. M., Sault R. J., Snowden S. L., 1999, MNRAS, 302, 417  
 Vázquez-Semadeni E., Ryu D., Passot T., González R., Gazol A., 2006, ApJ, 643, 245  
 Westpfahl D. J., Coleman P. H., Alexander J., Tongue T., 1999, AJ, 117, 868